Available online at www.sciencedirect.com

ScienceDirect

Ceramics International 39 (2013) 8761–8765

CERAMICS INTERNATIONAL

www.elsevier.com/locate/ceramint

The synthesis of single phase WC nanoparticles/C composite by solid state reaction involving nitrogen-rich carbonized polyaniline

Nemanja M. Gavrilov[a], Igor A. Pašti[a], Jugoslav Krstić[b], Miodrag Mitrić[c], Gordana Ćirić-Marjanović[a], Slavko Mentus[a,d,*]

[a]University of Belgrade, Faculty of Physical Chemistry, Studentski trg 12-16, 11158 Belgrade, Serbia
[b]University of Belgrade, Institute of Chemistry, Technology and Metallurgy, Njegoševa 12, 11001 Belgrade, Serbia
[c]University of Belgrade, Vinča Institute of Nuclear Sciences, P.O. Box 522, 11001 Belgrade, Serbia
[d]Serbian Academy of Sciences and Arts, Knez Mihajlova 35, 11000 Belgrade, Serbia

Received 28 February 2013; received in revised form 11 April 2013; accepted 17 April 2013
Available online 23 April 2013

Abstract

Single phase tungsten carbide nanoparticles (WC-NPs), (mean particle diameter 5.4 nm), distributed over carbonized polyaniline (C-PANI) nanotubes/nanosheets were synthesized by a solid state reaction between WO_3 and nitrogen-rich carbonized polyaniline at 1000 °C in a reducing atmosphere. The resulting composite was characterized by X-ray diffractometry, electron microscopy, thermogravimetry in oxidizing and reduction atmospheres and elemental analysis. We suggested that the synthesis of WC as a single phase was facilitated by reactive C atoms with dangling bonds, formed upon nitrogen removal.

Keywords: B. Nanocomposite; D. Tungsten carbide; Nitrogen depletion; Carbonized polyaniline

1. Introduction

Tungsten carbides (W_xC_y) were studied recently as promising supporting material for platinum catalysts in low-temperature fuel cells [1–3]. Their advantages were reported to be as follows: high stability, low electrical resistivity, strong Pt/support interaction and enhanced activity of Pt based electrocatalysts [3–5]. Usually tungsten carbide was prepared by solid-state reaction between a suitable tungsten source and graphitic carbon at temperatures above 1000 °C. This procedure yielded a mixture of phases such as low-valence W oxides (WO_x), WC and W_2C [6–9], while the large particle size caused relatively low specific surface area. Different approaches and tungsten precursors can be used to obtain single phase WC nanoparticles (WC-NPs), but the processes are sometimes very time-consuming. For instance, when scheelite ore was used as source of tungsten, its preparation by ball milling consumed 2–4 days [10,11]. The procedure using gas–solid reaction between the tungsten source and a hydrocarbon gas [1,12] allowed a reduction in both the time and temperature of synthesis. In addition, the synthesis procedure can be rationalized using a suitably chosen tungsten precursor [13]. Synthesis of phase-pure WC was also achieved using an electrical discharge machining followed by heat treatment of the resulting powder under N_2 or H_2 atmosphere [14].

Some authors achieved the enlargement of the specific surface area using supporting carbon of high surface area [1,5]. Various carbon materials were used for the synthesis purposes, involving Ketjen Black EC300J [1], ordered mesoporous carbon [2], carbon microspheres [4], Vulcan XC-72 [6] and carbon nanotubes (CNTs) [15]. Such prepared composites effectively expose WC-NPs to reacting media and ensure good electrical conductivity, making them suitable in various electrochemical applications.

In the synthesis of WC/carbon composites the thermal stability/inertness of carbon presents an important obstacle. The thermal stability of nitrogen-containing carbons was the

*Corresponding author at: University of Belgrade Faculty of Physical Chemistry Studentski trg 12 11158 Belgrade Serbia.
Tel./fax: +381 11 2187133.
E-mail address: slavko@ffh.bg.ac.rs (S. Mentus).

0272-8842/$ - see front matter © 2013 Elsevier Ltd and Techna Group S.r.l. All rights reserved.
http://dx.doi.org/10.1016/j.ceramint.2013.04.062

subject of several literature reports [16–19]. A decrease of nitrogen content upon heating was well documented for N-doped CNTs [16], N-doped graphene [17], C-PANI [18] and other nitrogen rich carbon types [19]. Assuming that the bond cleavage accompanying the removal of nitrogen from N-containing carbons may be beneficial for the carburization of tungsten, we attempted the WC synthesis by solid-state reaction of WO_3 with nitrogen-rich carbon obtained by carbonization of polyaniline. The WC-NPs/C-PANI nanocomposite involving single phase WC crystallites of very small mean radius (5.4 nm) was obtained successively at relatively low temperature and short time. The beneficial role of the initial content of N atoms in C-PANI precursor was emphasized.

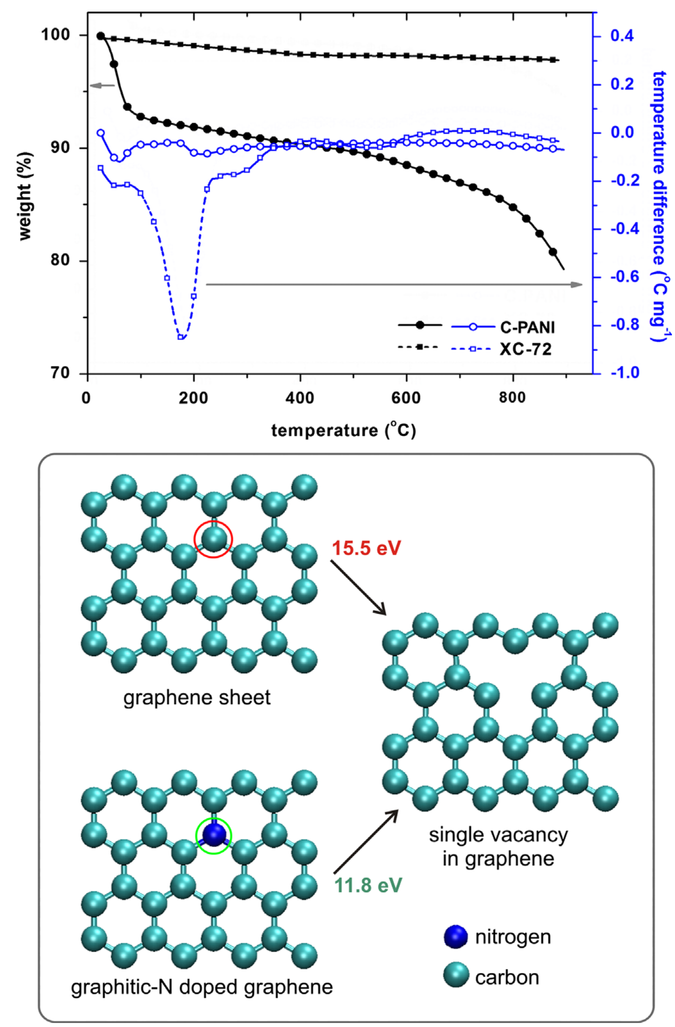

Fig. 1. TGA/DTA curves of C-PANI (circles) and Vulcan XC-72 (squares) in 5% H_2/Ar stream (top) and energy balance for removal of N and C atom from (graphitic N-doped) graphene sheet (bottom) estimated using DFT.

2. Experimental

Tungsten powder (Alfa Aesar) was dissolved in 30% H_2O_2, to obtain tungstic acid solution. Under continuous stirring, either the nanostructured C-PANI [20], or Vulcan XC-72, was added to this solution, with mass ratio against W of 9:1. By overnight drying at 80 °C, the precursors were obtained consisting of carbonaceous support impregnated with hydrated WO_3. The carburized materials, denoted as WC-NPs/C-PANI or W_xC_y/XC-72, were obtained by heating the precursors to 1000 °C at a rate of 10 °C min^{-1} in a reducing 5% H_2/Ar atmosphere, following by an isothermal treatment at 1000 °C for 4 h. The tungsten content in the resulting composite materials was determined by thermogravimetry (TG), upon combustion of the carbonaceous fraction under an air stream within a TA SDT 2960 thermobalance. To check the temperature stability of supporting carbons, the thermograms of C-PANI and Vulcan XC-72 under a stream of 5% H_2/Ar (both 99.9995 vol%) up to 900 °C were also recorded. Elemental analysis of both composite samples was carried out by Elemental Analyzer Vario EL III (Elementar). A scanning electron microscope (SEM) JEOL JSM 6460 LV was used to characterize the morphology of the samples. The X-ray powder diffractograms (XRD) were obtained on a Philips PW-1710 automated diffractometer using CuKα line. The mean crystallite diameter was calculated using the X-ray Line Fitting Program (XFIT) with a Fundamental Parameters convolution approach [21].

The periodic density functional theory (DFT) calculations were performed using PWscf code of QuantumESPRESSO distribution [22]. Full calculation details and model verification are provided in Supplementary data.

3. Results and discussion

The thermogravimetric stability test of C-PANI equilibrated with air, observed in a reducing atmosphere (Fig. 1, top), indicated the release of roughly 7% of the adsorbed water up to 100 °C, while mass loss commencing at around 500 °C, according to the literature [16–19], should be due to the nitrogen removal. The weight loss of around 9% between 500 and 900 °C matches closely the nitrogen content in C-PANI [20]. The elemental analysis (Table 1) confirmed a strong decrease in N/C ratio upon carburization (from 0.12 in C-PANI to 0.02 in WC-NPs/C-PANI). In addition, we confirmed by DFT calculations that the removal of the nitrogen atom from the graphene network is energetically favored in comparison with the removal of the C atom (Fig. 1, bottom). It is reasonable to expect that the defects formed in the C–C network, i.e., the C atoms with unsaturated, dangling bonds, accompanying the nitrogen removal become the reactive sites for further C–C bond breaking. A similar TG profile, confirming nitrogen removal from N-doped CNTs upon heating to 1000 °C in argon, was recently reported by Liu et al. [16], where also lower binding energy of pyridinic nitrogen relative to quaternary (graphitic) nitrogen was found. Heat treatment of N-doped graphene under a reducing atmosphere at 900 °C induced C–N bonds cleavage and removal of nitrogen [17]. The decrease in nitrogen concentration was found also upon the carbonization of partially carbonized C-PANI [18] and other nitrogen-rich carbons [19].

Table 1
Characteristics of prepared WC-NPs/C-PANI and W_xC_y/XC-72 samples obtained by XRD analysis, TG analysis and elemental microanalysis. Elemental composition of C-PANI is enclosed, too.

			WC-NPs/C-PANI	**W_xC_y/XC-72**	
XRD analysis	Present phases		WC	WC	ε-W_2C
	Relative amounts (%)		100	15	85
	Crystallite size (nm)		5.4	7.2	10.2
TG analysis	Tungsten mass fraction (%)		15.9	12.5	
Elemental composition[a] **(wt%)**	**Element**	**C-PANI**	**WC-NPs/C-PANI**	**W_xC_y/XC-72**	
	C	74.8	66.5	80.0	
	N	8.9	1.4	0.2	
	O	14.2	15.6	7.1	
	H	2.1	0.6	0.2	
	S	–	–	–	
	W	–	15.9	12.5	

[a]Obtained by compiling the results of elemental microanalysis (C, N, H, S) and thermogravimetric analysis (W), while oxygen content was determined by difference.

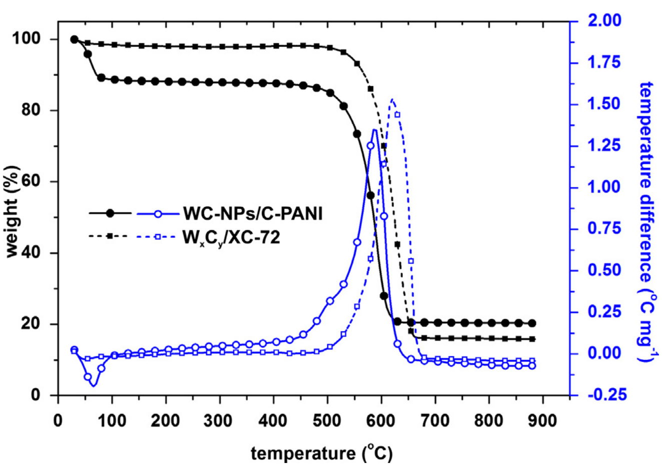

Fig. 2. TGA/DTA curves of WC-NPs/C-PANI and W_xC_y/XC-72 in air.

The thermogravimetric analysis of the synthesized composites in air atmosphere was carried out in order to determine the C:W mass ratio, and the results are presented in Fig. 2. Due to a much higher initial specific surface area of C-PANI in comparison with Vulcan (322 against 220 $m^2\,g^{-1}$ [6,23] the composite WC-NPs/C-PANI is more able to adsorb moisture, and the expulsion of moisture causes the initial mass loss of this composite, visible up to temperature 100 °C. Both composites are relatively resistant to oxidation in air up to 500 °C, however on further heating, a sudden combustion appears visible as an abrupt drop of the TG curve. The composite WC-NPs/C-PANI is more reactive with oxygen, most probably because of its higher specific surface area. As expected, the combustion is accompanied by an exothermic peak of the DTA curve. As a result of heating in air up to 650 °C, all carbon content is driven off in form of CO_2, while both WC-NPs/C-PANI and W_xC_y/XC-72 yielded pure WO_3 as a final residue. The 20.1 wt% of residue upon WC-NPs/C-PANI combustion corresponds to 15.9 wt% of metallic W, or to 16.9 wt% of WC in the composite. The 15.8 wt% of residue upon W_xC_y/XC-72 combustion corresponds to 12.5 wt% of metallic W or to 13.0 wt% of carbide mixture. In both cases, the increase in tungsten content, relative to its content of 10% in the precursor, overrates the predictions based on full moisture removal (maximum 7% in C-PANI, and almost negligible percent in Vulcan XC-72), and nitrogen removal from C-PANI. Upon normalization of the results of elemental analysis (Table 1), before and after carburization to a constant content of metallic tungsten (of 10 mass units), one may calculate that during carburization of a C-PANI+WO_3 composite a notable loss of carbon took place, approximately 2.6 mass units per unit of mass of tungsten. Actually, from the starting mass ratio C:W = 0.9 × 74.8:10 = 67.32:10, we obtained the composite with a final mass ratio C:W = 66.5:15.9 = 41.8:10, where, according to the mass ratio in WC, only a small fraction, 0.65:41.15, of carbon was chemically bonded, while the majority was in an elemental state in the composite. The loss in carbon 67.32–41.8 = 25.5 per 10 mass units of W, may be attributed to the reaction of the supporting carbon material, partly with WO_3, and, in a greater part, with the oxygen traces in the flushing gas. According to the TG stability test in Fig.1, the main loss of carbon is expected to take place during the isothermal treatment of the precursor samples at 1000 °C, and its minimization appears to be rather a technical than a fundamental problem. A relative increase in O concentration was registered in each of the carburized samples, which may indicate the diffusion of oxygen from WO_3 toward the bulk of supporting carbon material.

XRD analysis of WC-NPs/C-PANI (Fig. 3) revealed diffraction patterns of pure hexagonal WC phase. This indicated complete conversion of WO_3 to WC. From the line broadening, crystallite size of WC-NPs was determined to amount to 5.4 nm. When Vulcan XC-72 was used as a precursor, the phase mixture W_2C (85%) and WC (15%) was obtained, while mean crystallite size amounted to 7.2 and 10.2 nm, for WC and W_2C, respectively.

The SEM picture of WC-NPs/C-PANI (Fig. 4) showed that this composite retained the morphology of original C-PANI (nanotubes/nanosheets, [23]), with slight sintering as a

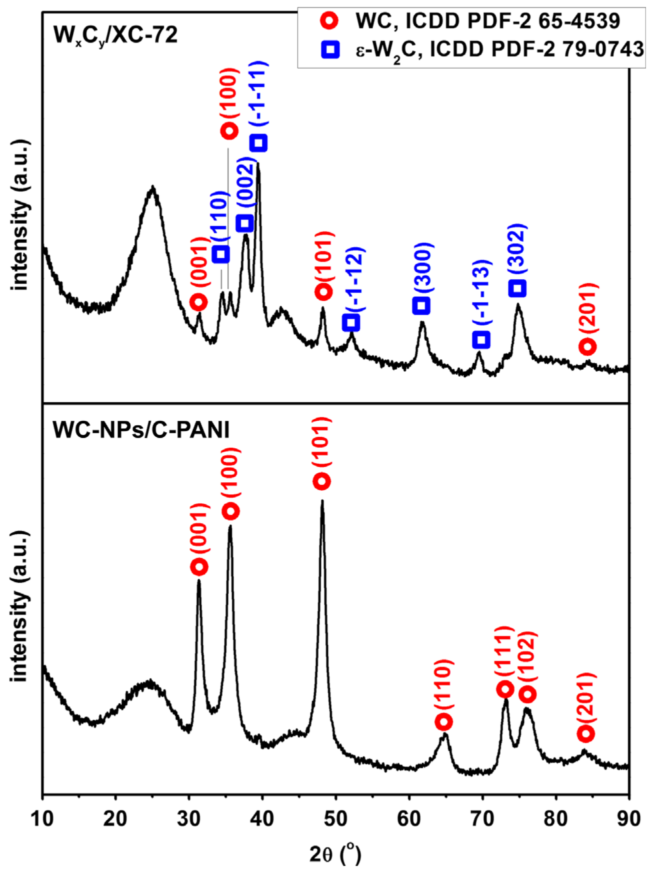

Fig. 3. XRD patterns of W_xC_y/XC-72 (top) and WC-NPs/C-PANI (bottom).

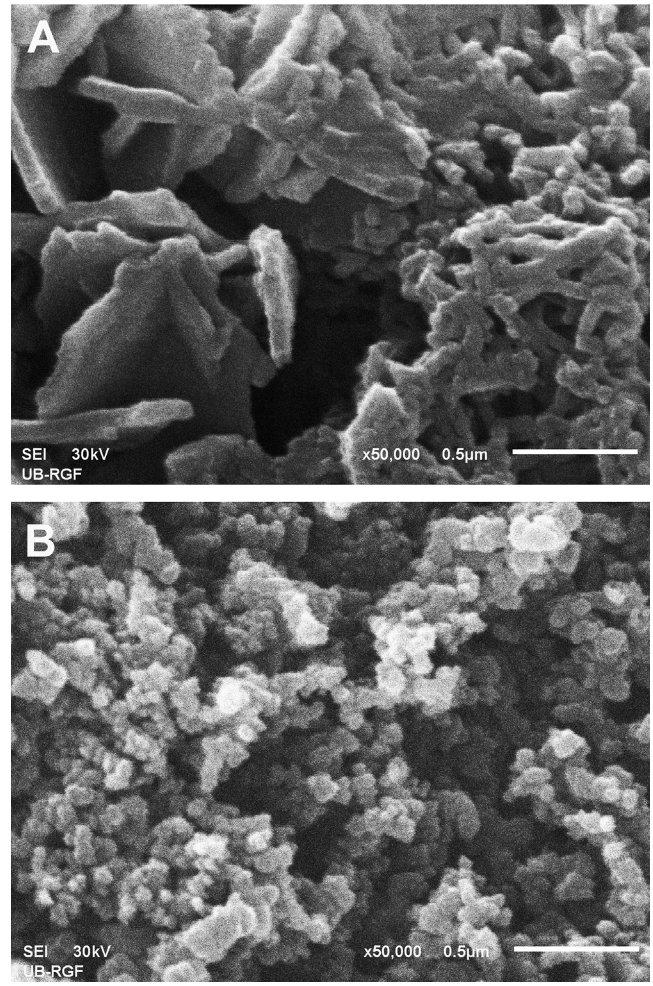

Fig. 4. SEM images of the WC-NPs/C-PANI (A) and W_xC_y/XC-72 (B).

consequence of carburization. The SEM picture of W_xC_y/XC-72 indicated uniform granules roughly 50 nm in diameter, (Fig. 3), corresponding to an original morphology of Vulcan XC-72 which has been documented many times so far. The SEM images reveal globules with an average diameter of approximately 50 nm [24–26]. This indicates that morphology of Vulcan XC-72 is not changed upon carburization.

The composition of the final carbide phase depends on the formation rate of an activated carbon atom (C*) and its diffusivity through tungsten [12]. Slow formation of C* and its fast diffusion through the metallic W enable W_2C to be first formed. If diffusion of C* is slow, a WC shell forms around the W core. Thus, assuming the rate of C* diffusion to be independent of the carbon source, the conclusion may be derived that C-PANI promotes the fast formation of a large number of C* atoms above 500 °C, especially in the range 700–900 °C, where WO_x in the precursor was predominantly reduced to metallic tungsten [12]. This may be considered to favor WC formation and to reduce the synthesis temperature. Surface functional groups of C-PANI were identified and quantified previously using XPS [23,27]. Since pyridinic nitrogen contributes with ~35% in the total nitrogen content in C-PANI [23,27], WC formation at lower temperatures is favored in view of the fact that pyridinic nitrogen displayed higher reactivity relative to other types of nitrogen in the carbon source [16]. The heteroatoms (N and O), if present in the carbon source, help to spread the tungsten source uniformly over the carbon surface during precursor formation, and consequently, favor high dispersion of W_xC_y, as we confirmed in this study.

4. Conclusions

Nitrogen-rich carbon was used for the first time to prepare WC/C composite. Phase pure WC-NPs, with mean crystallite size of 5.4 nm, were deposited on C-PANI by direct reduction in an H_2/Ar stream where nitrogen rich C-PANI served as both the carbon source and the support. Nitrogen atoms incorporated in a carbon network of C-PANI are removed at elevated temperatures (above 500 °C) thus promoting the formation of a large number of activated carbon atoms, facilitating, we suggest, successful WC-NPs formation. A reductive gaseous atmosphere led to a reduced sacrificial loss of carbon. Based on our findings, nitrogen-rich carbon can be used for a facile synthesis of phase-pure WC-NPs at relatively low temperatures. This could provide a route for a low cost mass production of WC-NPs/carbon composites for various applications, such as electrocatalysis and charge storage.

Acknowledgment

This work was supported by the Serbian Ministry of Education and Science (Contracts III45014, OI172043 and III45001). S.V.M. acknowledges the support provided by the Serbian Academy of Sciences and Arts through the project "Electrocatalysis in the contemporary processes of energy conversion".

Appendix A. Supporting information

Supplementary data associated with this article can be found in the online version at http://dx.doi.org/10.1016/j.ceramint.2013.04.062.

References

[1] M. Shao, B. Merzougui, K. Shoemaker, L. Stolar, L. Protsailo, Z.J. Mellinger, et al., Tungsten carbide modified high surface area carbon as fuel cell catalyst support, Journal of Power Sources 196 (2011) 7426–7434.

[2] Y. Wang, C. He, A. Brouzgou, Y. Liang, R. Fu, D. Wu, et al., A facile soft-template synthesis of ordered mesoporous carbon/tungsten carbide composites with high surface area for methanol electrooxidation, Journal of Power Sources 200 (2012) 8–13.

[3] W. Zhu, A. Ignaszak, C. Song, R. Baker, R. Hui, J. Zhang, et al., Nanocrystalline tungsten carbide (WC) synthesis/characterization and its possible application as a PEM fuel cell catalyst support, Electrochimica Acta 61 (2012) 198–206.

[4] Y. Wang, S. Song, V. Maragou, P.K. Shen, P. Tsiakaras, High surface area tungsten carbide microspheres as effective Pt catalyst support for oxygen reduction reaction, Applied Catalysis B 89 (2009) 223–228.

[5] H. Chhina, S. Campbell, O. Kesler, High surface area synthesis, electrochemical activity, and stability of tungsten carbide supported Pt during oxygen reduction in proton exchange membrane fuel cells, Journal of Power Sources 179 (2008) 50–59.

[6] E.J. Rees, C.D.A. Brady, G.T. Burstein, Solid-state synthesis of tungsten carbide from tungsten oxide and carbon, and its catalysis by nickel, Materials Letters 62 (2008) 1–3.

[7] J.B. Joo, J.S. Kim, P. Kim, J. Yi, Simple preparation of tungsten carbide supported on carbon for use as a catalyst support in a methanol electro-oxidation, Materials Letters 62 (2008) 3497–3499.

[8] J. Ma, S.G. Zhu, Direct solid-state synthesis of tungsten carbide nanoparticles from mechanically activated tungsten oxide and graphite, International Journal of Refractory Metals and Hard Materials 28 (2010) 623–627.

[9] K. Essaki, E.J. Rees, G.T. Burstein, Influence of precursor preparation on the synthesis of WC under microwave irradiation, Materials Letters 63 (2009) 2185–2187.

[10] H. Singh, O.P. Pandey, Direct synthesis of nanocrystalline tungsten carbide from scheelite ore by solid state reaction method, Ceramics International 39 (2013) 785–790.

[11] H. Singh, O.P. Pandey, Single step synthesis of tungsten carbide (WC) nanoparticles from scheelite ore, Ceramics International, in press,.

[12] R. Koc, S.K. Kodambaka, Tungsten carbide (WC) synthesis from novel precursors, Journal of the European Ceramic Society 20 (2000) 1859–1869.

[13] H. Lin, B. Tao, J. Xiong, Q. Li, Y. Li, Tungsten carbide (WC) nanopowders synthesized via novel core–shell structured precursors, Ceramics International 39 (2013) 2877–2881.

[14] M.-H. Lin, Synthesis of nanophase tungsten carbide by electrical discharge machining, Ceramics International 31 (2005) 1109–1115.

[15] N. Keller, B. Pietruszka, V. Keller, A new one-dimensional tungsten carbide nanostructured material, Materials Letters 60 (2006) 1774–1777.

[16] H. Liu, Y. Zhang, R. Li, X. Sun, H. Abou-Rachid, Thermal and chemical durability of nitrogen-doped carbon nanotubes, Journal of Nanoparticle Research 14 (2012) 1016.

[17] X. Li, H. Wang, J.T. Robinson, H. Sanchez, G. Diankov, H. Dai, Simultaneous Nitrogen-Doping and Reduction of Graphene Oxide, arXiv:0910.0862 [cond-mat.mtrl-sci].

[18] G. Ćirić-Marjanović, I. Pašti, N. Gavrilov, A. Janošević, S. Mentus, Carbonised polyaniline and polypyrrole: towards advanced nitrogen-containing carbon materials, Chemical Papers, in press, http://dx.doi.org/10.2478/s11696-013-0312-1.

[19] E.J. Ra, E. Raymundo-Pinero, Y.H. Lee, F. Beguin, High power supercapacitors using polyacrylonitrile-based carbon nanofiber paper, Carbon 47 (2009) 2984–2992.

[20] S. Mentus, G. Ćirić-Marjanović, M. Trchová, J. Stejskal, Conducting carbonized polyaniline nanotubes, Nanotechnology 20 (2009) 245601.

[21] R.W. Cheary, A.A. Coelho, A fundamental parameters approach to X-ray line-profile fitting, Journal of Applied Crystallography 25 (1992) 109–121.

[22] P. Giannozzi, S. Baroni, N. Bonini, M. Calandra, R. Car, C. Cavazzoni, et al., QUANTUM ESPRESSO: a modular and open-source software project for quantum simulations of materials, Journal of Physics: Condensed Matter 21 (2009) 395502.

[23] N. Gavrilov, I. Pašti, M. Vujković, J. Travas-Sejdic, G. Ćirić-Marjanović, S. Mentus, High-performance charge storage by N-containing nanostructured carbon derived from polyaniline, Carbon 50 (2012) 3915–3927.

[24] J.H. Bang, K. Han, S.E. Skrabalak, H. Kim, K.S. Suslick, Porous carbon supports prepared by ultrasonic spray pyrolysis for direct methanol fuel cell electrodes, Journal of Physical Chemistry C 111 (2007) 10959–10964.

[25] G. Wu, L. Li, J.-H. Li, B.-Q. Xu, Polyaniline-carbon composite films as supports of Pt and PtRu particles for methanol electrooxidation, Carbon 43 (2005) 2579–2587.

[26] K.-W. Park, Y.E. Sung, S. Han, Y. Yun, T. Hyeon, Origin of the enhanced catalytic activity of carbon nanocoil-supported PtRu alloy electrocatalysts, Journal of Physical Chemistry B 108 (2004) 939–944.

[27] N. Gavrilov, I.A. Pašti, M. Mitrić, J. Travas-Sejdić, G. Ćirić-Marjanović, S.V. Mentus, Electrocatalysis of oxygen reduction reaction on polyaniline-derived nitrogen-doped carbon nanoparticle surfaces in alkaline media, Journal of Power Sources 220 (2012) 306–316.